2010

Analysis of the Vane Contact Force and the Vane Side Friction Loss of the Various Revolving Vane Expander Designs

Alison Subiantoro
School of Mechanical and Aerospace Engineering

Kim Tiow Ooi
School of Mechanical and Aerospace Engineering

Analysis of the Vane Contact Force and the Vane Side Friction Loss of the Various Revolving Vane Expander Designs

Alison SUBIANTORO[1]*, Kim Tiow OOI[2]

Nanyang Technological University,
School of Mechanical & Aerospace Engineering,
Thermal & Fluids Engineering Division,
Singapore
[1]+65 6790 4674, alis0004@ntu.edu.sg,
[2]+65 6790 5511, mktooi@ntu.edu.sg

ABSTRACT

The performances of the four possible RV expander design configurations at suction pressures of 2, 6 and 10 bars and a 1 atm discharge pressure with air as the working fluid are studied in this paper. The study was carried out theoretically by analyzing the vane contact forces and the vane side friction losses behaviors. It was found that the expander design with the vane fixed at the rotor and when the rotor is the driving component configuration (RV-I) produces the best performance, irrespective of the operating pressures. On the other hand, the expander design with the vane at the cylinder and when the rotor is the driving component (RV-IIa) consistently produces the worst performance. It was also found that the vane contact forces and the vane side friction losses are mainly affected by the inertia of the driving component and not by the operational pressures.

1. INTRODUCTION

In response to the findings on how man-made refrigerants used in refrigeration, heating and air-conditioning systems affect the environment, Lorentzen and Pettersen (1993) proposed to use CO_2 as a potential future refrigerant. Due to the thermophysical properties of CO_2, a system based on a transcritical cycle was proposed. However, due to the large operating pressure range, the system usually has a large throttling loss resulting in low energy efficiency. To overcome this issue, Lorentzen (1994) proposed to recover energy from the throttling loss by replacing the conventional expansion valve with an expander. Robinson and Groll (1998) found that by using an expander, a 25% increase in the COP of the CO_2 refrigeration system can be achieved.

Since then, many types of expanders based on the existing compressor designs have been proposed (Nickl *et al.*, 2005, Kim *et al.*, 2008, Kovacevic *et al.*, 2006, Fukuta *et al.*, 2009, Matsui *et al.*, 2009). Recently, a new type of compressor named the revolving vane (RV) compressor was introduced by Teh and Ooi (2009a, 2009b). The mechanism has also been used for an expander (Subiantoro and Ooi, 2009).

RV mechanism falls under the rotary machine category. However, while in most designs, a stationary cylinder is used, both the rotor and the cylinder rotate together in this mechanism. This reduces the relative velocities of all the components, resulting in lower friction losses, producing the aforementioned superior performance. Further observations on the revolving vane mechanism show that there are at least four possible configurations available. They are:

1. RV-I: The vane is attached to the rotor and the rotor is the driving component (Figure 1(a)).
2. RV-Ia: The vane is attached to the rotor and the cylinder is the driving component (Figure 1(b)).
3. RV-II: The vane is attached to the cylinder and the cylinder is the driving component (Figure 1(c)).
4. RV-IIa: The vane is attached to the cylinder and the rotor is the driving component (Figure 1(d)).

Subiantoro and Ooi (2010) have shown that RV-I is superior as compared to RV-II when used as expanders in a transcritical CO_2 system. It is also realized in the study that the vane contact forces of both the RV-Ia and RV-IIa designs are functions of the pressure difference across the vane, unlike the RV-I and RV-II designs. Therefore, in high pressure applications like the transcritical CO_2 refrigeration system, RV-Ia and RV-IIa are inferior as compared to RV-I and RV-II. However, there is no reported study in low pressure applications yet.

It is the purpose of this paper to study the compare the performances of the four possible RV expander designs in relatively low pressure applications (lower than 10 bars). The vane contact force and the vane side friction loss will be used as the main indicator of the performance. A good expander should have low vane contact force and low friction loss. In addition, the peak of the vane contact force should ideally occur when the vane exposed length is not too long in order to minimize stress experienced by the vane. The investigations will be carried out theoretically.

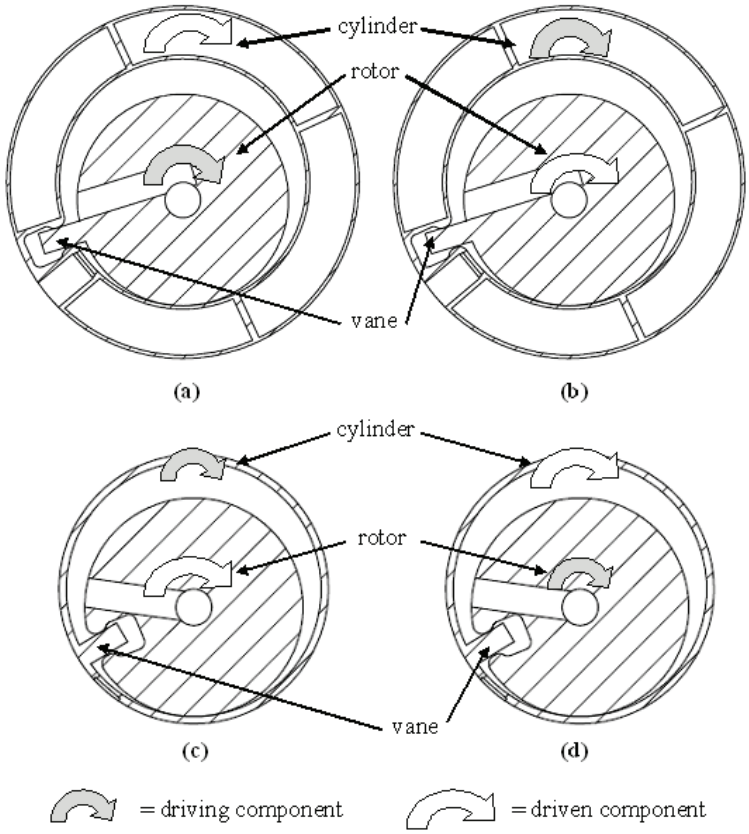

Figure 1: Alternative RV mechanism designs: (a) RV-I, (b) RV-Ia, (c) RV-II, (d) RV-IIa

2. THEORETICAL MODEL

To conduct the investigations, the expander chambers are assumed to be perfectly sealed and adiabatic. The driving component of the expander turns at a constant angular speed. The vane thickness is assumed to have negligible effects to the kinematics of the expander. An ideal suction valve is used. The valve is assumed to open instantaneously when the expander operating angle is zero and closes instantaneously when the expansion is about to begin. The timing of the start of the expansion is decided based on the isentropic expansion assumption.

For simplicity and as the effect is fluid independent, air is used as the working fluid and the air properties are obtained using the REFPROP routine (Lemmon *et al.*, 2007). Three different suction pressure conditions, i.e. 2 bar, 6 bar and 10 bar, were tested. The discharge pressure is fixed at the atmospheric condition. The main dimensions of the expander and main operating conditions parameters are shown in Table 1.

Table 1: Main dimensions of the expander and main operating condition parameters

Rotor radius	18 mm
Cylinder radius	25 mm
Expander length	32 mm
Rotor rotating inertia	0.0002 kg.m^2
Cylinder rotating inertia	0.0002 kg.m^2
Driving component speed	3000 rpm
Friction coefficient	0.15
Suction temperature	25 ºC
Discharge pressure	101325 Pa
Discharge temperature	25 ºC

During operation, the vane rubs against the vane slot. This rubbing process causes the vane side friction loss. This power loss can be calculated according to Equation (1).

$$P_{v,f} = \eta_v F_{v,n} \frac{dl_v}{dt} \tag{1}$$

The vane contact forces of RV-I, RV-Ia, RV-II and RV-IIa can be calculated using equations (2a)-(2d), respectively.

$$F_{v,n,I} = \frac{I_{c,I}\alpha_{c,I} + \sum T_{c,I}}{r_c \cos\gamma_I - \eta_v\left(r_c \sin\gamma_I - \frac{w_v}{2}\right)} \tag{2a}$$

$$F_{v,n,Ia} = \frac{\Delta p_{Ia} l_e l_{v,Ia}\left(r_r + \frac{l_{v,Ia}}{2}\right) - I_{r,Ia}\alpha_{r,Ia} - \sum T_{r,Ia}}{\left(r_r + l_{v,Ia}\right) + \eta_v \frac{w_v}{2}} \tag{2b}$$

$$F_{v,n,II} = \frac{I_{r,II}\alpha_{r,II} + \sum T_{r,II}}{r_r \cos\gamma_{II} - \eta_v\left(r_r \sin\gamma_{II} + \frac{w_v}{2}\right)} \tag{2c}$$

$$F_{v,n,IIa} = \frac{\Delta p_{IIa} l_e l_{v,IIa}\left(r_c - \frac{l_{v,IIa}}{2}\right) - I_{c,IIa}\alpha_{c,IIa} - \sum T_{c,Iia}}{\left(r_c - l_{v,Iia}\right) + \eta_v \frac{w_v}{2}} \tag{2d}$$

Equations (2a) and (2b) show that the RV-I and RV-II contact forces depend on the inertia and the other losses (i.e. the endface and the bearing losses) components. However, they are independent of the pressure force acting across the vane. On the other hand, Equations (2c) and (2d) show that the contact forces for the RV-Ia and RV-IIa are dependent on the pressure, the inertia and the other losses components. It is also interesting to note that the pressure component and the other terms in equations (2b) and (2d) are of the opposite signs.

A computer code using the FORTRAN programming language was created to simulate the processes involved in the system. These include the kinematics, thermodynamics and the dynamics processes. The simulation was performed with a 0.0005 radian operating angle step. The kinematics processes were first simulated to produce all the

kinematics parameters such as the driven component angle, angular velocity and angular acceleration. These parameters were then used to simulate the thermodynamics processes. The results from both processes were then used to simulate the dynamics processes to produce the dynamics parameters including the vane contact force and the vane side friction power loss.

3. RESULTS AND DISCUSSIONS

The angular accelerations of the driven components of the four possible RV expander designs are shown in Figure 2.

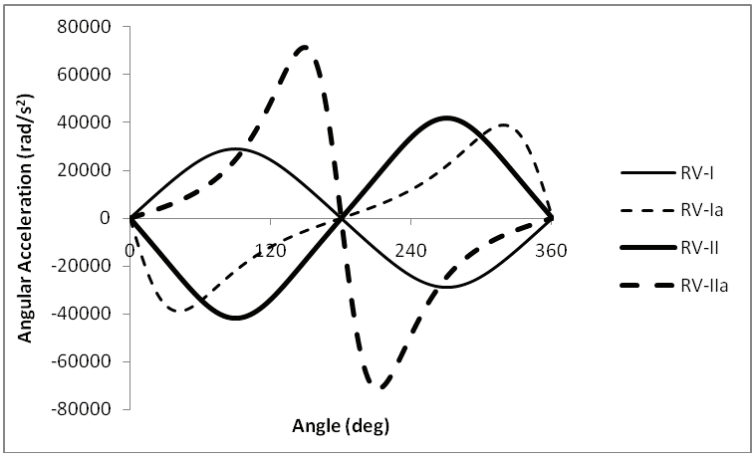

Figure 2: Angular accelerations of the driven components of the four possible RV expander designs

The angular accelerations of the driven components behave in a sinusoidal manner, unlike the pressure component which is always positive. Therefore, it is expected that although the pressure and the inertia components of the vane contact forces in Equations (2b) and (2d) have opposite signs, they can only cancel each other for half of the cycle. They will then magnify the vane contact forces together for the other half of the cycle.

Figure 2 also shows that the amplitude of the acceleration of the driven component of RV-I is the smallest while the amplitude of RV-IIa is the largest. The peaks are located at different operating angles. The peaks of RV-I and RV-II lie around the mid-points of the first and the second halves of the cycles. The peaks of RV-Ia lie around the beginning and the end of the operating cycle, while they are near the mid-point of the cycle in RV-IIa.

The variations of the vane contact forces for the 2 bar, 6 bar and 10 bar suction pressures are shown in Figures 3-5.

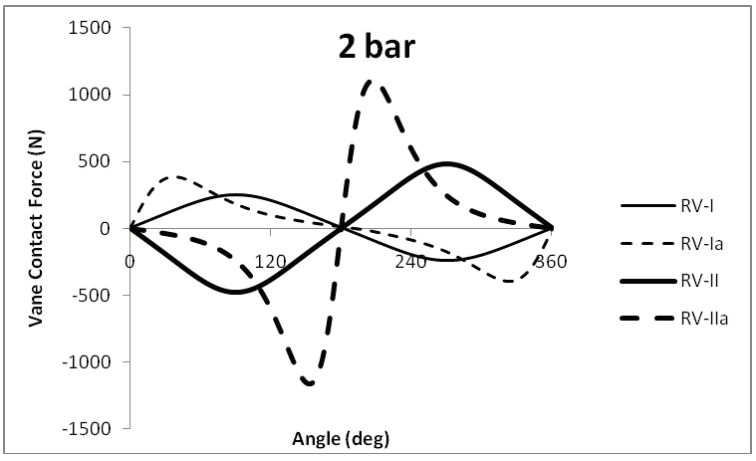

Figure 3: Vane contact forces of the four possible RV expander designs at 2 bar suction pressure

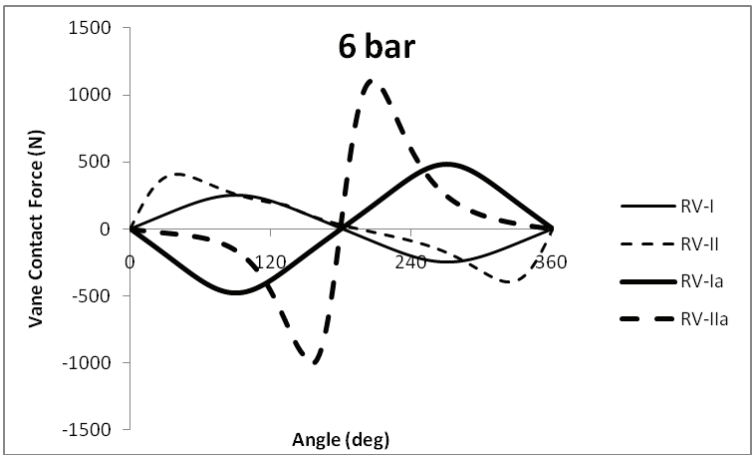

Figure 4: Vane contact forces of the four possible RV expander designs at 6 bar suction pressure

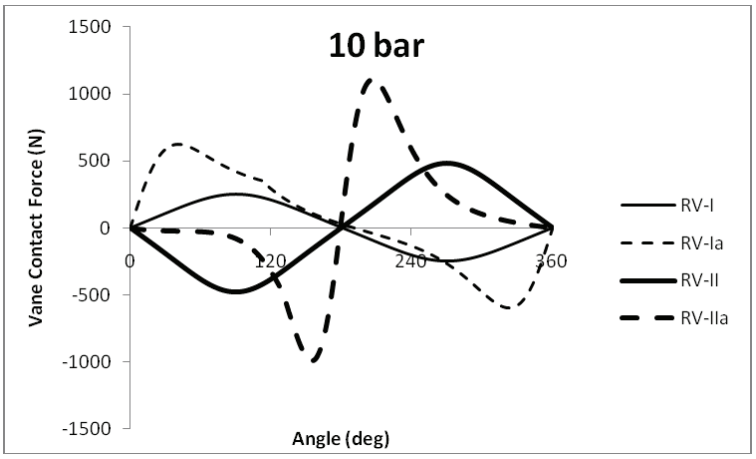

Figure 5: Vane contact forces of the four possible RV expander designs at 10 bar suction pressure

Figures 3-5 show that the vane contact forces are mainly affected by the acceleration, not the pressures. This is because they follow the behaviors of the angular accelerations very closely, even for the RV-Ia and RV-IIa configurations. Only at relatively high pressures, the effects of pressure to the vane contact forces are observable. This is most obvious in the 10 bar suction pressure case. The RV-Ia vane contact force is observably increased by the pressure while the RV-IIa vane contact force is observably decreased by the pressure for the first half of the operation in the 10 bar case. As for the other half of the cycle, the pressure effects are not too obvious because the high pressure gas has been expanded and so the pressure across the vane is no longer as high as the first half.

The locations of the peaks of the RV-Ia vane contact forces are most desirable because they lie near the beginning and the end of the operating cycle, when the vane exposed length is shortest. The locations of the peak contact forces for RV-IIa are the worst. They lie near the mid-point of the cycle where the vane exposed length is the longest. This indicates that the vane of the RV-IIa design will experience the highest bending stress as compared to the other three designs.

Figures 3-5 also show that in agreement with the acceleration profile shown in Figure 2, the amplitude of the vane contact force of the RV-I design is consistently the smallest while the amplitude of RV-IIa is consistently the largest. It is interesting to observe that the amplitude of the vane contact force of RV-Ia is smaller than RV-II when the suction pressure is 2 or 6 bar, but is larger when the suction pressure is 10 bar.

The vane side friction power losses of the four possible RV expander designs at suction pressures of 2, 6 and 10 bar are shown in Figures 6-8 respectively.

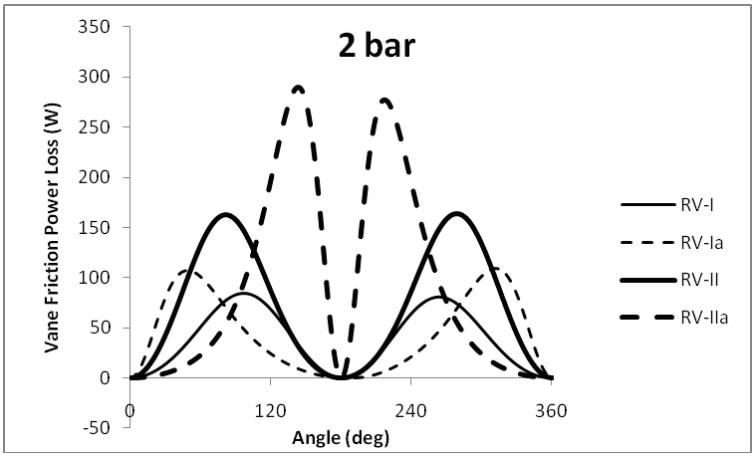

Figure 6: Vane side friction power losses of the four possible RV expander designs at 2 bar suction pressure

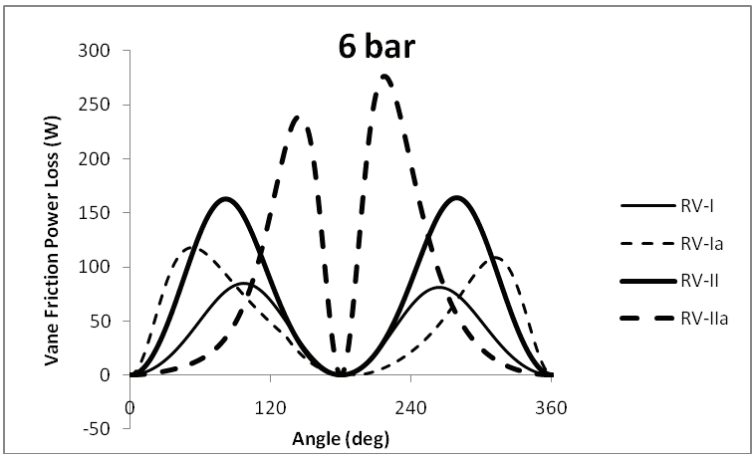

Figure 7: Vane side friction power losses of the four possible RV expander designs at 6 bar suction pressure

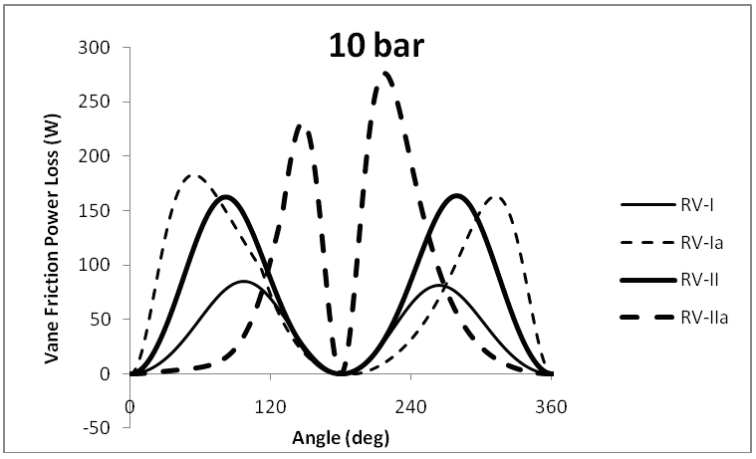

Figure 8: Vane side friction power losses of the four possible RV expander designs at 10 bar suction pressure

From Figures 6-8, we can see that RV-I always gives the lowest vane friction average power loss while RV-IIa always produces the largest vane friction average power loss, irrespective of what the suction pressure is. Consistent with the vane contact forces behaviors, the vane contact force of RV-Ia is smaller than RV-II when the suction pressure is 2 or 6 bar but is larger than RV-II when the suction pressure is 10 bar.

The observable differences in the two peaks of the RV-Ia and the RV-IIa vane friction power losses are due to the pressure effect. Therefore, the differences are not so obvious when the suction pressure is 2 bar and they become more obvious as the suction pressure increases.

It is useful to observe the behaviors of the vane sliding velocities as shown in Figure 9 to better understand the behaviors of the vane side friction power losses.

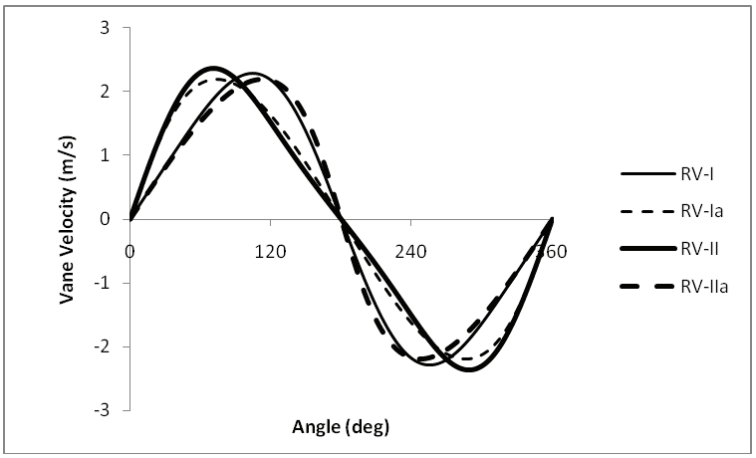

Figure 9: Vane sliding velocities of the four possible RV expander designs

Figure 9 shows that the peaks of the vane sliding velocities of the RV-I and most importantly the RV-IIa designs are closer to the mid-point of the full operating cycle than the other two designs. This means that in the RV-IIa design, the peaks of the angular acceleration of the driven component, which are also the peaks of the vane contact forces, and the peaks of the vane sliding velocities coincide with each other. This is not the case in the other three designs. Coupling this and the fact that RV-IIa has the largest vane contact force amplitude results in RV-IIa having the largest amplitude of the vane friction power loss among the four designs as shown in Figure 6-8.

4. CONCLUSIONS

A theoretical study has been conducted to compare the performances of the four possible RV expander configuration designs by observing the vane contact forces and the vane side friction losses. The study was carried out at suction pressures of 2, 6 and 10 bars. The results show the RV-I configuration, where the vane is fixed at the rotor and rotor is the driving component, shows the least energy loss with lowest vane side contact force. On the other hand, the RV-IIa configuration design, where the vane is at the cylinder and rotor is the driving component, consistently produces the worst performance. These findings are irrespective of the operating pressure conditions. Another notable finding is that the locations of the maximum vane contact forces of RV-Ia are most desirable since they occur when the vane exposed lengths are short. It was also found that the pressure across the vane does not contribute significantly to the vane contact forces and the vane side friction losses when the suction pressure is 2 bar. However, as the suction pressure increases, the effect becomes more obvious, albeit still small due to the relatively low operating pressures studied here.

NOMENCLATURE

F	force	(N)	**Subscripts**	
I	rotating inertia	($kg.m^2$)	I	RV-I
l	length	(m)	Ia	RV-Ia
p	pressure	(Pa)	II	RV-II
P	power	(W)	IIa	RV-IIa
r	radius	(m)	c	cylinder
t	time	(s)	e	expander
T	torque	(Nm)	f	friction
w	width	(m)	n	normal
α	angular acceleration	(rad/s^2)	r	rotor
γ	angle between rotor and cylinder radii at vane contact	(rad)	v	vane
η	friction coefficient	(-)		

REFERENCES

Fukuta, M., Yanagisawa, T., Higashiyama, M., Ogi, Y., 2009, Performance of Vane-Type CO2 Expander and Characteristics of Transcritical Expansion Process. *HVAC&R Res.*, vol. 15, no. 4: p. 711-727.

Kim, H.J., Ahn, J.M., Cho, S.O., Cho, K.R., 2008, Numerical Simulation on Scroll Expander-Compressor Unit for CO2 Trans-Critical Cycles. *Appl. Therm. Eng.*, vol. 28, no. 13: p. 1654-1661.

Kovacevic, A., Stosic, N., Smith, I.K., 2006, Numerical Simulation of Combined Screw Compressor-Expander Machines for Use in High Pressure Refrigeration Systems, *Simul. Model. Pract. Th.*, vol. 14, no. 8: p. 1143-1154.

Lemmon, E.W., Huber, M.L., McLinder, M.O., 2007, NIST Standard Reference Database 23: Reference Fluid Thermodynamic and Transport Properties-REFPROP, *National Institute of Standards and Technology, Standard Reference Data Program*.

Lorentzen,G., Pettersen, J., 1993, A New, Efficient and Environmentally Benign System for Car Air-Conditioning, *Int. J. Refrig*., vol. 16, no. 1: p. 4-12.

Lorentzen, G., 1994, Revival of Carbon Dioxide as a Refrigerant, *Int. J. Refrig.*, vol 17, no. 5:p. 292-301.

Matsui, M., Ogata, T., Wada, M., Wasegawa, H., 2009. Development of the High-Efficiency Technology of a CO2 Two-Stage Rotary Expander. *HVAC&R Res.*, vol. 15, no. 4: p. 743-758.

Nickl, J., Will, G., Quack, H., Kraus, W.E., 2005, Integration of a Three-Stage Expander into a CO_2 Refrigeration System, *Int. J. Refrig.*, vol. 28, no. 8: p. 1219-1224.

Robinson, D.M., Groll, E.A., 1998. Efficiencies of Transcritical CO_2 Cycles With and Without an Expansion Turbine, *Int. J. Refrig.*, vol. 21, no. 7: p.577-589.

Subiantoro, A., Ooi, K.T., 2009, Introduction of the Revolving Vane Expander. *HVAC&R Res.*, vol. 15, no. 4: p. 801-816.

Subiantoro, A., Ooi, K.T., 2010, Design Analysis of the Novel Revolving Vane Expander in a Transcritical Carbon Dioxide Refrigeration System, *Int. J. Refrig.*, doi: 10.1016/j.ijrefrig.2009.12.023.

Teh, Y.L., Ooi, K.T., 2009a, Theoretical Study of a Novel Refrigeration Compressor - Part I: Design of the Revolving Vane (RV) Compressor and Its Frictional Losses, *Int. J. Refrig*., vol. 32, no. 5: p. 1092-1102.

Teh, Y.L., Ooi, K.T., 2009b, Experimental Study of the Revolving Vane (RV) Compressor, *Appl. Therm. Eng.*, vol. 29, no. 14-15: p. 3235-3245.